

Polar Kerr-Effect Observation of Perpendicular Surface Anisotropy for Ultrathin fcc Fe Grown on Cu(100)

C. Liu, E. R. Moog, and S. D. Bader

Materials Science Division, Argonne National Laboratory, Argonne, Illinois 60439

(Received 26 February 1988)

The predicted perpendicular surface anisotropy is observed for ferromagnetic fcc Fe/Cu(100) via *in situ* polar Kerr-effect measurements. Square hysteresis loops are obtained for films 1.5 to 5.7 monolayers thick for 100-K growth. The region of stability of the perpendicularly magnetized state as a function of growth temperature and film thickness is delineated. Combined longitudinal and polar Kerr-effect measurements show that the anisotropy reverts to being in plane for films thicker than ≈ 6 monolayers.

PACS numbers: 75.70.-i, 75.30.Gw, 75.30.Pd, 78.20.Ls

A major challenge in the field of surface magnetism is to test the predictions of perpendicular surface anisotropy for monolayer (ML) range Fe films.^{1,2} Experimental efforts focused on this issue have used ferromagnetic resonance,³ Mössbauer spectroscopy,⁴ Brillouin scattering,⁵ and spin-polarized photoemission,^{2,6,7} using Fe epitaxially deposited on Ag(100) (Refs. 2-6) and Cu(100) (Ref. 7) and in sandwich and superlattice structures (Ref. 5). While there are studies that confirm⁴ or extrapolate³ to perpendicular easy axes in the ultrathin limit, there are others that suggest that perpendicular-orientation stability occurs in an intermediate thickness range.^{6,7} For the fcc Fe/Cu(100) studied in Ref. 7, the trend with film thickness was contrary to expectation: A 5-ML-thick film exhibited perpendicular anisotropy, but 3- and 1-ML-thick films did not. This observation has been related to the controversial surface structural question: To what extent can ideal atomic-layer epitaxy be achieved in the laboratory?^{8,9} In this Letter we systematically investigate Fe/Cu(100) to determine the range of growth conditions that supports perpendicular anisotropy. This information provides a clear picture of the competing influences of the nonequilibrium kinetic and intrinsic physical processes that act to determine the magnetic properties of these novel heterostructures.

The films were grown in 10^{-11} -Torr ultrahigh vacuum (UHV) and characterized by LEED-Auger and magneto-optic Kerr-effect measurements as in previous studies.¹⁰ New experimental features of the present study include the fact that the growth-temperature regime was extended down to ≈ 100 K from previous values of ≈ 460 K. This led to substantially broadened LEED beams, as expected. The applied magnetic fields were increased from previous limits (≈ 200 Oe) to the present maximum of 1.7 kOe. Also, polar, and crossed polar and longitudinal, Kerr configurations were adopted to monitor perpendicular and parallel (in-plane) spin orientations, respectively, while only the longitudinal signal was monitored previously. Tapered vanadium Permendur electromagnet poles in the UHV chamber allow the *p*-

polarized light beam from an intensity-stabilized He-Ne laser to reflect off the sample. To generate magnetic hysteresis loops the change in the intensity of the light that passes through an analyzing crystal polarizer is monitored as the applied field is swept. This intensity component is referred to as the Kerr intensity I_K ; it is proportional to the Kerr rotation and to the sample magnetization. Typical hysteresis curves are accumulated in less than 3 min, in which time signals from ≈ 20 scans are averaged.

The hysteresis loops of Fig. 1 are polar Kerr-effect results for a 4.2-ML fcc Fe film grown epitaxially on Cu(100) at ≈ 100 K and measured at the indicated temperatures as the film warmed up. The squareness of the loops at the lower temperatures indicates single-domain-type switching with the remanent-state magnetization $I_K(H=0)$ having the same value as at high fields, $I_K(H_{\max})$. Three types of easy axes are considered in discussion of the interpretation of Fig. 1. First, shape anisotropy can dictate an in-plane orientation. Second, surface anisotropy can dictate a perpendicular orientation. And, last, a canted orientation (not in plane and not perpendicular) completes the range of possibilities. An in-plane orientation is ruled out because of the perpendicular geometry. A canted orientation cannot be ruled out as readily because it could give rise to a magnetization component that projects along the surface normal, and also because the $\{111\}$ directions are canted and are known to be easy axes for bulk fcc ferromagnets. However, such canted structures are ruled out because (a) the longitudinal Kerr signal indicated that the film could not be magnetized with remanence by an in-plane field, and (b) the observation from the polar measurements that $I_K(H=0) = I_K(H_{\max})$ indicates that the magnetization direction was not rotated from the canted towards the normal direction as the field was increased, as would be expected for a canted structure. Thus, we conclude that the results of Fig. 1 are unambiguously due to perpendicular anisotropy governing the magnetization direction of the fcc-Fe/Cu(100) film.

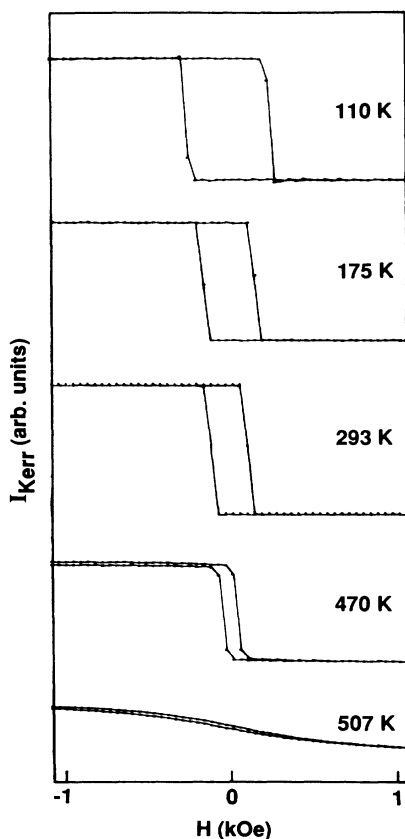


FIG. 1. Polar Kerr-effect hysteresis curves for 4.2-ML-thick fcc Fe grown epitaxially on Cu(100) at ≈ 100 K. The data were taken at the indicated temperatures as the sample warmed up. The square loops show that the easy axis of magnetization is perpendicular to the film plane.

Figure 2 shows the thickness dependence of I_K and the coercivity H_c for films grown, held, and measured at ≈ 100 K. The films all exhibited square-loop behavior. The increase in the I_K signal with thickness indicates that each Fe layer contributes *ferromagnetically* to the total signal. This rules out the possibility that the film is antiferromagnetic, as predicted by self-consistent band-structure calculations^{10,11} and as observed for fcc Fe precipitates at the grain boundaries of Cu-rich alloys.¹² The initial slope of the I_K signal is smaller than that extrapolated back from the thicker-film region, as indicated by the two straight dashed lines through the data. This and the trend in the H_c data suggest that the properties of the first monolayers may be different from that of the "average" layer. This could be due to the intrinsic electronic structure of the interface¹¹ and/or to compositional gradients at the interface^{8,9} due to intermixing of the Cu and Fe.

Thermal-cycling studies were performed, as shown in Fig. 3, to evaluate the role of intermixing. For a monolayer-range film grown at ≈ 100 K, cycled to elevated temperatures, and cooled back down, as shown

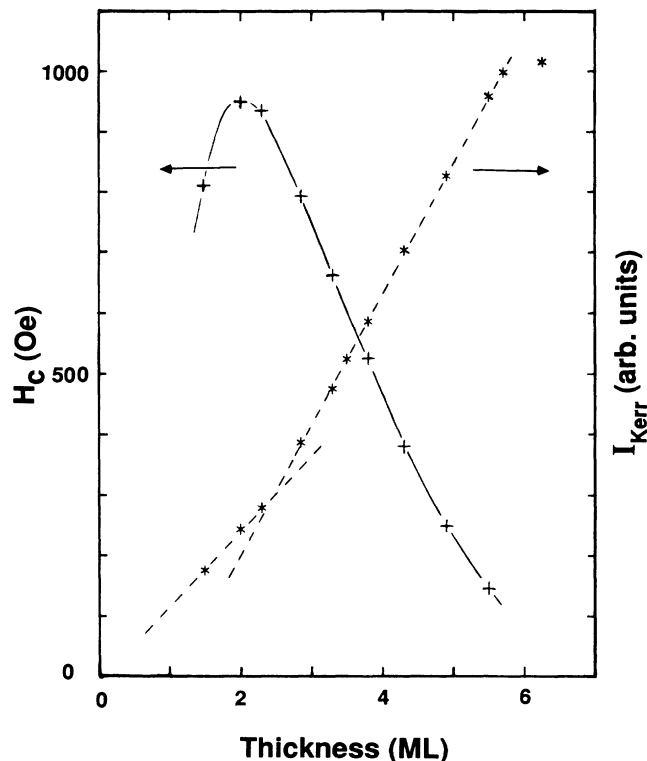


FIG. 2. Thickness dependence of the polar Kerr intensity I_K and the coercivity H_c for fcc Fe/Cu(100) grown and measured at ≈ 110 K. All films exhibit perpendicular anisotropy except the 6.2-ML film. The dashed lines through the data are guides to the eye.

sequentially in Fig. 3(a), the original square loop is not recovered. But for a multilayer cycled in similar manner there are no irreversible changes between 100 K and room temperature, and only modest changes, as shown in Fig. 3(b), due to cycling above room temperature. This indicates that the intermixing that is thermally promoted is strictly confined to the first interfacial monolayers in these studies.

Figure 4 outlines the region of stability of the perpendicular anisotropy. The operational definition of stability is the observation of square hysteresis loops in the polar Kerr-effect measurements. The temperature ordinate corresponds to the constant temperature of the film during growth *and* Kerr-effect measurement. Perpendicular anisotropy is observed for a relatively broad range of film thicknesses for growth at low temperatures as compared to higher temperatures. This may be understood as resulting from a competition of two types of processes. First, perpendicular spin orientations are not realized in the monolayer-thickness limit even at 100 K because of the nonideal interface morphology. As temperature is raised, the thickness range of the interfacial mixing increases, so that the onset of the square-loop behavior moves to higher Fe dosages, as is shown by the left-hand-side boundary in Fig. 4. Second, the anisotropy

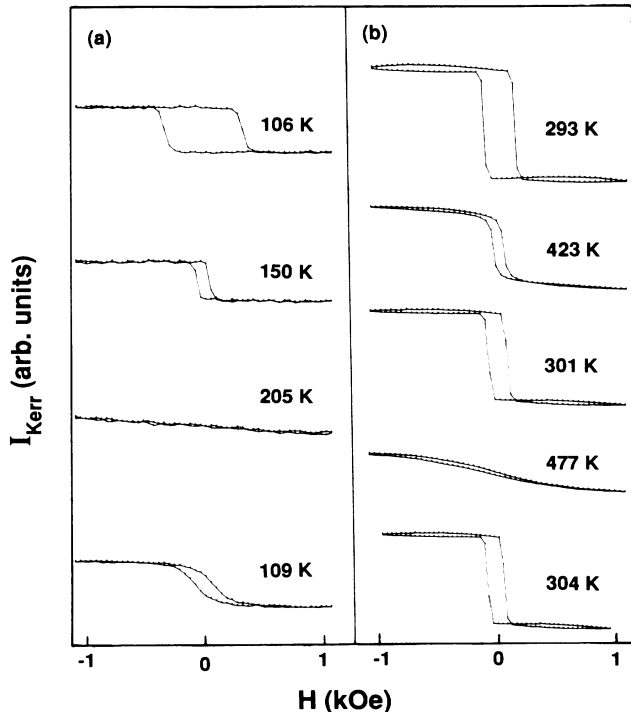


FIG. 3. Thermal-cycling sequences from top to bottom for (a) 1.5-ML- and (b) \approx 4-ML-thick fcc Fe/Cu(100) grown at \approx 100 K. The low-temperature hysteresis curve for the 1.5-ML film changes irreversibly upon warming to \approx 240 K because of interfacial intermixing.

(and coercivity) weakens substantially as temperature increases [e.g., see Figs. 1 and 3(b)]. This causes the upper limit of film thickness that is controlled by perpendicular anisotropy to decrease as growth temperature increases, as is shown by the upper right-hand-side boundary of Fig. 4.

The boundaries of stability in Fig. 4 can be used to elucidate the systematics presented in Ref. 7. The films in that study were grown near the temperature of the peak in the stability diagram of Fig. 4, and so only one film thickness exhibited perpendicular anisotropy; thicker and thinner films did not. Similar observations⁶ were made for Fe/Ag(100). (Note that the diffusion effects at the interface cause the boundaries of stability actually to be influenced by time-temperature considerations.) For the higher-temperature regime for fcc Fe/Cu(100), not shown in Fig. 4, a weak, nonsaturating polar Kerr signal was observed,¹³ as expected from the results of Ref. 10.

For film thicknesses in excess of those along the right-hand-side boundary in Fig. 4, the easy axis has reoriented itself in the plane of the film. This is in accord with our attributing the perpendicularly magnetized state to the predicted^{1,2} perpendicular *surface* anisotropy. It is clear that the $\{111\}$ canted directions do not become the easy axes, from the observation that the longitudinal Kerr effect shows open-loop switching with substantial

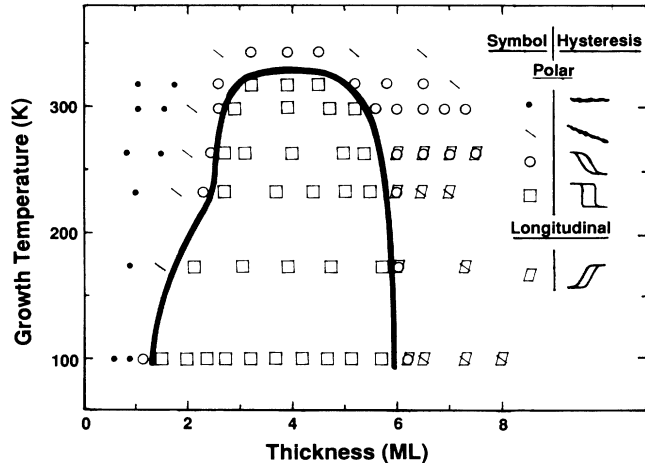


FIG. 4. The region of stability of perpendicular anisotropy for fcc Fe/Cu(100) outlined on a plot of film thickness vs growth temperature. The Kerr-effect measurements used to determine the stability boundaries were made at the growth temperature.

remnance, while the polar Kerr effect does not. For $[111]$ easy-axis orientation both Kerr-effect configurations would be expected to show qualitatively similar behavior.

As a final point, we consider the stability conditions for perpendicular orientation when temperature is raised *subsequent* to growth. This constitutes another dimension of the stability plot of Fig. 4. We have found that perpendicularly oriented films grown at low temperature can retain their easy axes [e.g., see Figs. 1 and 3(b)] when the temperature is raised to values in excess of those that define the upper growth-temperature boundary in Fig. 4. We attribute this incremental enhancement in the stability to a growth-induced anisotropy contribution associated with the increased roughness inferred from our LEED results for low-temperature-grown films. Annealing such films to 350 K, for instance, still yields broader LEED-beam profiles¹³ than those of films grown at 350 K. The anneal influences, but does not remove, the roughness. Thus, it is intriguing to emphasize that surface roughness, as well as a suppression of interfacial mixing, may critically influence the anisotropy.

In summary, the Kerr effect has provided a direct observation of perpendicular surface anisotropy of an ultrathin Fe film: fcc Fe/Cu(100). The thickness and growth-temperature dependence of stability of the perpendicularly-oriented state was delineated. Longitudinal Kerr-effect measurements performed sequentially on the same films provided supporting evidence to confirm the spin orientations of the films. Thermal-cycling studies provided a direct indication of the role of and extent to which interfacial mixing influences the magnetic properties.

This work was supported by the U.S. Department of

Energy, Office of Basic Energy Sciences, Division of Materials Sciences, under Contract No. W-31-109-ENG-38. We thank J. Pearson for technical assistance.

-
- ¹J. G. Gay and R. Richter, *Phys. Rev. Lett.* **56**, 2728 (1986).
²B. T. Jonker, K.-H. Walker, E. Kisker, G. A. Prinz, and C. Carbone, *Phys. Rev. Lett.* **57**, 142 (1986).
³B. Heinrich, K. B. Urquhart, A. S. Arrott, J. F. Cochran, K. Myrtle, and S. T. Purcell, *Phys. Rev. Lett.* **59**, 1756 (1987).
⁴N. C. Koon, B. T. Jonker, F. A. Volkening, J. J. Krebs, and G. A. Prinz, *Phys. Rev. Lett.* **59**, 2463 (1987).
⁵J. R. Dutcher, B. Heinrich, J. F. Cochran, D. A. Steigerwald, and W. F. Egelhoff, Jr., *J. Appl. Phys.* **63**, 3464 (1988).
⁶M. Stampanoni, A. Vaterlaus, M. Aeschlimann, and F. Meier, *Phys. Rev. Lett.* **59**, 2483 (1987).
⁷D. Pescia, M. Stampanoni, G. L. Bona, A. Vaterlaus, R. F. Willis, and F. Meier, *Phys. Rev. Lett.* **58**, 2126 (1987).
⁸S. A. Chambers, T. J. Wagener, and J. H. Weaver, *Phys. Rev. B* **36**, 8992 (1987).
⁹D. A. Steigerwald and W. F. Egelhoff, Jr., *Surf. Sci.* **192**, L887 (1987).
¹⁰P. A. Montano, G. W. Fernando, B. R. Cooper, E. R. Moog, H. M. Naik, S. D. Bader, Y. C. Lee, Y. N. Darici, H. Min, and J. Marcano, *Phys. Rev. Lett.* **59**, 1041 (1987).
¹¹C. L. Fu, A. J. Freeman, and T. Oguchi, *Phys. Rev. Lett.* **54**, 2700 (1985); C. L. Fu and A. J. Freeman, *Phys. Rev. B* **35**, 925 (1987).
¹²Y. Tsunoda, N. Kunitomi, and R. M. Nicklow, *J. Phys. F* **17**, 2447 (1987).
¹³C. Liu, E. R. Moog, and S. D. Bader, unpublished.